Convolutional Neural Network for Convective Storm Nowcasting Using 3D Doppler Weather Radar Data

Lei Han, Juanzhen Sun, Wei Zhang*

***Abstract*—Convective storms are one of the severe weather hazards found during the warm season. Doppler weather radar is the only operational instrument that can frequently sample the detailed structure of convective storm which has small spatial scale and short lifetime. For the challenging task of short term convective storm forecasting (i.e., nowcasting), 3D radar images contain information about the processes in convective storm. However, effectively extracting such information from multi-source raw data has been problematic due to a lack of methodology and computation limitations. Recent advancements in deep learning techniques and Graphic Processing Units (GPUs) now make it possible. This study investigates the feasibility and performance of an end-to-end deep learning nowcasting method. The nowcasting problem was transformed into a classification problem first, and then a deep learning method that uses a convolutional neural network (CNN) was presented to make predictions. On the first layer of CNN, a cross-channel 3D convolution was proposed to fuse 3D raw data. The CNN method eliminates the handcrafted feature engineering, i.e. the process of using domain knowledge of the data to manually design features. Operationally-produced historical data of the Beijing–Tianjin–Hebei region in China was used to train the nowcasting system and evaluate its performance. 3,737,332 samples were collected in the training dataset. The experimental results show that the deep learning method improves nowcasting skill compared with traditional machine learning methods.**

***Index Terms*—Weather radar, deep learning, convolutional neural network, convective storm forecasting**

I. Introduction

Convective storms are hazardous warm-season events that may include hail, lightning and strong wind. The short-term forecasting (i.e. nowcasting) of these systems remains a challenge. Due to its small spatial scale and short duration, it is difficult for the conventional observing instruments to carry out effective monitoring. Because of the high spatial and temporal resolution, Doppler weather radar is the only operational instrument that can frequently sample the detailed 3D structure of convective storm [1].

Unlike longer-term weather forecasting, numerical weather prediction (NWP) models are not of much use for nowcasting for the first few hours, especially for the first hour [1]. Therefore, various radar-based nowcasting algorithms have been developed to assist forecasters in the warning process of severe weather [2]. Besides weather radar data, a high resolution data assimilation model system can now provide valuable information about unobserved meteorological variables which can be used to assist in nowcasting. Including re-analysis data can help to improve the forecasting of convective initiation or fast storm growth which is hard for methods only using radar data. In the Beijing 2008 Forecast Demonstration Project (B08FDP), the Olympic forecasters manually used the low-level wind and temperature provided by the four-dimensional Variational Doppler Radar Analysis System (VDRAS) to forecast storm initiation and growth [3]. Several studies have indicated that developing advanced methods that can extract valuable information directly from the raw data is the key to making the best use of these multi-source datasets [4-6]. However, this has been problematic due to a lack of methodology and computation limitations. Recent advances in deep learning techniques and GPUs (Graphic Processing Units) provide another means for the development of new techniques for nowcasting convective storms. In this paper, we describe a nowcasting method based on deep learning and evaluate its performance in nowcasting convective storms.

Traditional nowcasting methods rely on algorithms that extrapolate radar observations of storm echoes or expert systems that synthesize multi-source data based-on predefined rules [1, 3]. For example, SCIT (Storm Cell Identification and Tracking; [7]) and TITAN (Thunderstorm Identification, Tracking and Nowcasting; [8]) use techniques that can identify and track individual storms and produce nowcasts based on tracking information and its extrapolation. TREC (Tracking Reflectivity Echoes by Correlation; [9-10]) uses optical flow techniques that compute motion vectors in order to extrapolate radar echoes. An example of an expert system is the Auto-Nowcaster (ANC; [11]), which combines various observations, NWP model output, climatological data, and a radar-based tracking algorithm to produce nowcasts using a fuzzy logic method. In addition to tracking existing storms, ANC also attempts to nowcast convective storm initiation.

The performance of traditional nowcasting methods is lim-

*** (*Corresponding author: Wei Zhang*.)**

L. Han and W. Zhang are with College of Information Science and Engineering, Ocean University of China, Qingdao 266100, China (email: hanlei@ouc.edu.cn; weizhang@ouc.edu.cn)

J. Sun is with National Center for Atmospheric Research, Boulder, CO 80301, U.S. (email: sunj@ucar.edu)

ited by their underlying physical assumptions. For example, extrapolation methods assume that storm evolution is linear and ANC uses a conceptual model based on boundary layer convergence lines to nowcast convective initiation (CI). These assumptions only partially represent the true atmospheric state. In contrast, machine learning methods can extract predictive information from data without making any physical assumptions. Han et al. made an attempt to develop a machine learning nowcasting method without such assumptions, called the support vector machine box-based nowcasting (SBOW) method [12]. SBOW can learn predictive knowledge from the historical data of the four-dimensional Variational Doppler Radar Analysis System (VDRAS) [13]. In addition to skillfully predicting storm propagation, SBOW also showed potential for predicting storm initiation and growth. However, a shortcoming of SBOW is the manual construction of temporal and spatial features (i.e., handcraft feature engineering). In general, handcraft feature engineering is a time-consuming process that depends heavily on expert guidance. With the large amount of observational radar data and meteorological re-analysis data generated daily, it is anticipated that useful feature representations can be learned directly from these raw data without the need for handcraft feature engineering.

Advances in deep learning methods now make it possible for such an application. Several deep learning methods, such as stacked denoising autoencoders (SDAE), deep belief network (DBN) and convolutional neural network (CNN), have been developed [14-21]. See [17] for an overview of deep learning techniques. Deep learning methods are typically expected to perform better than shallow machine learning methods (such as SBOW) because of their end-to-end abstract ability and multi-layered feature representation. Starting from raw data, these methods compute a layer-wise transformation of each representation, producing abstract levels with increasingly improved feature representation. By using a series of these transformations, complex feature representations can be learned automatically without the use of handcraft feature engineering. Successful applications of deep learning techniques have been demonstrated in various fields such as image and speech recognition and the prediction of new drug molecules [17]. Tao et al. applied a deep learning method (SDAE) to improve the quality of satellite precipitation products based on two-dimensional infrared images [6, 22, 23]. Shi et al. proposed a convolutional long short-term memory network which used consecutive 2D radar reflectivity images to extrapolate future radar images [24]. Their method achieved better performance than an optical flow-based method but still have difficulties in convective initiation forecasting.

In this study, we first transform the nowcasting problem into a classification problem and then present a deep learning method that uses CNN to make predictions. Operationally-produced historical data from the region of Beijing – Tianjin – Hebei in China are used to train the deep learning system and evaluate its performance. We then demonstrate the skill of CNN-based nowcasting.

This paper is organized as follows. Section 2 describes the data used in this study. Section 3 describes the architecture of the CNN deep learning method. Section 4 presents the experimental results. Discussion and conclusions are presented in Section 5.

II. DATA

The weather radar works in three dimensions as shown in Fig. 1 [7]. The radar scans from the lowest elevation angle and gradually increases the angle (5~14 angles according to different scan strategies). On each elevation angle, the interval of adjacent radials is ~1°. The spatial resolution is 1 km. So the output of one scan on an elevation angle is a 2-D image, and all 2-D images created on different elevation angles constitute a 3D image. The time interval of two successive 3D images is typically 5~6 minutes. The remotely sensed data obtained by Doppler weather radar include reflectivity, radial velocity and spectrum width. Radar reflectivity data is often used by extrapolation methods to make forecasts. Radial velocity is mainly used in wind structure analysis which may be further used in some numerical models. As the original polar coordinate is inconvenient for analysis, the reflectivity data is often interpolated into a Cartesian coordinate [8].

All radar images and model re-analysis data used in this study are collected by the Beijing Meteorological Service (BMS) in China. The radar images are a three-dimensional mosaic from six operational radars over the Beijing – Tianjin – Hebei region including four S-band radars (BJRS in Beijing city, TJRS in Tianjin city, SJZRS in Shijiazhuang city, and QHDRS in Qinhuangdao city) and two C-band radars (ZBRC in Zhangbei county and CDRC in Chengde city). The spatial resolution is 1 km and the temporal frequency is 6 minutes. The six radars include four S-band radars and two C-band radars from the network of the China Next Generation Weather Radars (CINRADs). Their locations, along with the study domain and provincial/metropolitan borders, are shown in Fig. 2. The radar mosaic technique is described in Chen et al. [25].

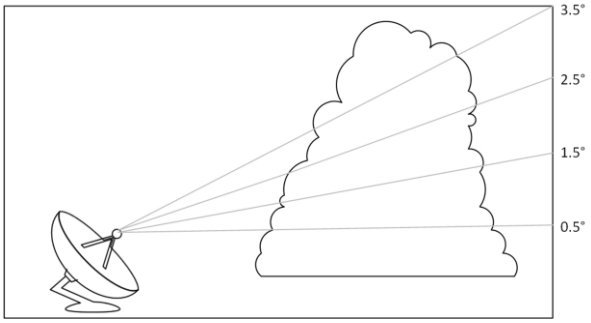

Fig. 1. Illustration of how a weather radar remotely senses atmospheric objects. The radar scans from the lowest elevation angle and gradually increases the angle.

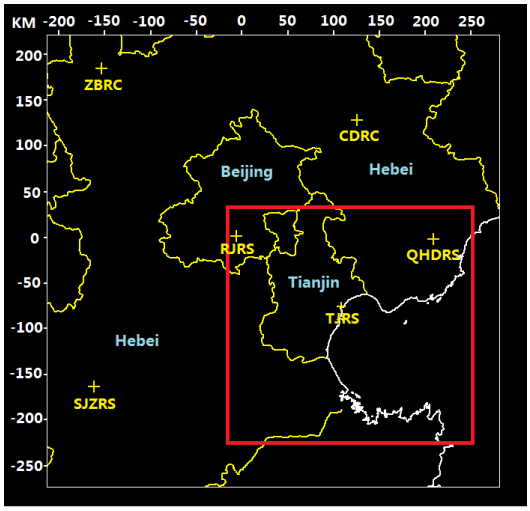

Fig. 2. The study domain (red rectangle), covering most of Tianjin, part of Beijing, and part of Hebei. The yellow lines indicate the provincial/metropolitan borders and the white line indicates the costal line. The locations of the six radars are shown by the yellow cross.

Meteorological re-analysis data produced by data assimilation model systems can provide valuable atmospheric background information which can be used to assist in nowcasting convective initiation [12]. VDRAS is a high-resolution model which can assimilate data from surface observations, mesoscale model data and radar observations [13, 26]. By including a cloud-scale numerical model and the adjoint of the mesoscale numerical model, VDRAS can retrieve valuable lower-atmosphere unobserved meteorological variables like wind and temperature. VDRAS has been used widely throughout the world and is an effective tool for forecasters to manually analyze atmospheric background information. VDRAS data is used in this study to assist in nowcasting along with radar data. All VDRAS data we used are also collected by BMS. The VDRAS data has the grid resolution of 3 km in the horizontal direction and 500 m in the vertical direction. The VDRAS re-analysis is produced at 10 to 15 minute intervals, according to the arrival times of radar observations. Finally, all radar and VDRAS data are interpolated onto a common grid with a horizontal resolution of 0.01° in the geospatial coordinate. We use the data collected from June to July 2015 for training and validation, while the data collected in August for testing.

III. Methodology

We divide the study domain into many position-fixed small boxes (0.06° × 0.06°, about 6 × 6 km) and the nowcasting problem is transformed into a binary classification problem, i.e., will a radar echo ⩾ 35 dBZ appear in a box in 30 minutes? For radar data, for example, it has 6 × 6 × 20 pixels in this 3D box. Fig. 3 presents an overview of the deep learning algorithm used in this study. It should be noted that the 35 dBZ is chosen as a threshold for the purpose of developing and evaluating the method and other threshold values can be selected depending on user's need.

During the training period, historical 3D radar images and model re-analysis data are fed directly into the CNN network to train a two-class classifier (i.e., 0 or 1). The trained classifier is then used to make predictions on new data. If the classifier's output in a given box at time t is 1, it means that radar echoes ⩾ 35 dBZ (i.e., a convective storm) will be present at time t + 30 minutes. If the output is 0, there is no convective storm in the box. All boxes classified as 1 will be marked as red rectangle. Compared with traditional machine learning methods, the deep learning method eliminates the need for manual feature construction, making the process automatic; i.e., so-called "end-to-end" machine learning. Here "end to end" means we directly feed the raw 3D radar and VDRAS data into our network without handcraft feature engineering, which is often a complicated and time-consuming process in traditional machine learning methods like SBOW. Note that the SDAE or DBN methods are more suitable for one- or two-dimensional data. The CNN method we use is more appropriate for the 3D multivariate data in this study.

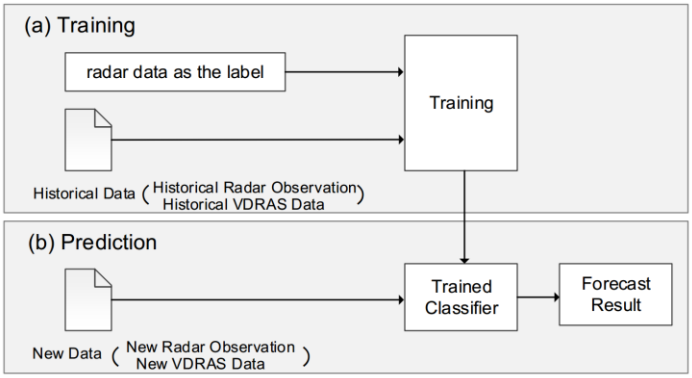

Fig. 3. Flowchart of the proposed deep learning algorithm. The historical 3D radar images and model re-analysis data are fed directly into the CNN network to train a two-class classifier during the training period. The trained classifier is then used to make predictions on new data.

A. Architecture of Convolutional Neural Network

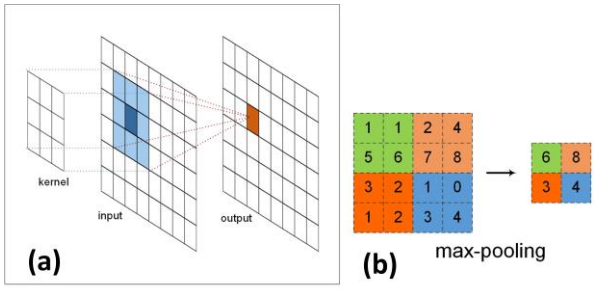

Fig. 4. Schematic illustration of convolution and pooling. (a). A kernel is used to slide over the input image to obtain an output, i.e. feature map. (b). The max-pooling outputs the maximum value of each patches indicated by different colors.

A well-recognized advantage of CNN is that it uses local connectivity to learn global patterns. This is done by two operations: convolution and pooling. By stacking sequential layers of convolution and pooling, a CNN network can be constructed. The purpose of the convolution is to extract features from the input data. It preserves the spatial relationship between pixels by learning features from small subsets of input

data. Each neuron of a convolutional layer is connected to a small region in the input data. The connection of this small region is called the kernel or filter. This architecture ensures that the learned filters produce the strongest response to local input patterns. A feature map can then be obtained by moving a filter over the input image (as shown in Fig. 4(a)). A number of feature maps are produced after each convolution.

Therefore, these two variables and their temporal trends (*pt*, *dpt*, *w*, *dw*) are chosen as the input variables, where *pt* stands for perturbation temperature (proportional to buoyancy), *w* is the vertical velocity, and *dpt* and *dw* are the temporal trends. The raw data associated with these variables provided by VDRAS are then fed into the convolutional neural network. Because of the different temporal resolutions between the radar and

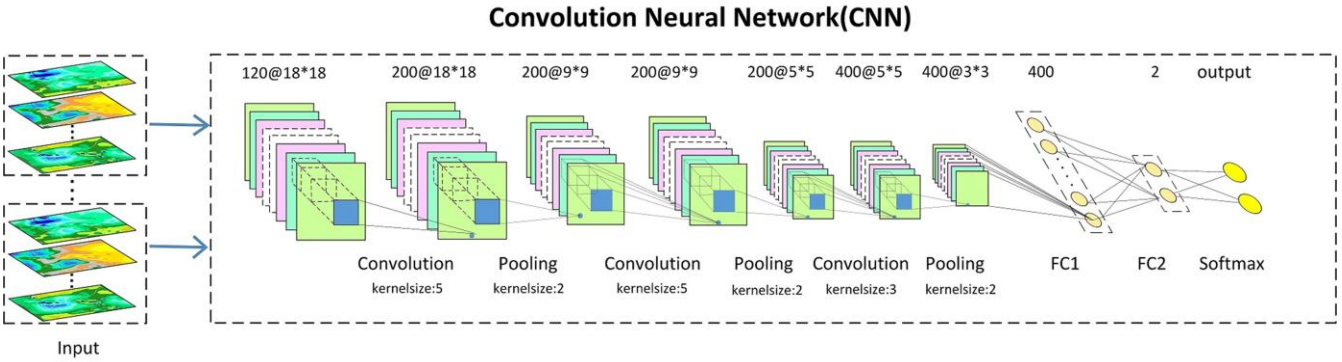

Fig. 5. The architecture of the convolutional neural network used in this study. 120@18*18 in the first layer means we stack 6 channel 3D data (each channel has 20 vertical levels, and each level has the size of 18*18). 200@18*18 in the second layer means we get 200 feature maps (shown as stacked rectangles). The numbers in other layers are similar.

Pooling is the process of down-sampling by outputting the maximum or average of non-overlapping regions (as shown in Fig. 4 (b)). The purpose of pooling is to reduce the dimensionality of each feature map while retaining critical information. The pooling operation also reduces the size and improves the manageability of the input representations. Finally, pooling reduces the number of parameters and computations in the network through which overfitting could be controlled.

Fig. 5 shows the overall CNN architecture used in this study. The CNN has three convolutional layers and three pooling layers. There are two fully connected (FC) layers connected to the last feature map. The kernel size is 5×5 while 3×3 is used for the last convolutional layer. A stochastic gradient descent (SGD) algorithm is used for learning with the learning rate of 0.001. The number of parameters is roughly 2.32 million; training is conducted on a Tesla GPU. Note that the network used here is different from those 2-D convolution neural networks since the first layer is cross-channel 3D convolution which will be discussed in section 3.3.

B. Establishing the Training Dataset

As radar observations have been widely used for convective weather forecasting, here we use radar reflectivity *R* and its temporal trend *dR* as CNN's input. *dR* is the point-to-point difference:

$$dR = R_t - R_{t-1}$$

Since it is hard to predict convective initiation (CI) and evolution if we only use radar observations [3], we add VDRAS re-analysis data because it can provide useful lower-atmosphere meteorological fields such as temperature and wind, which are important factors to determine convective storm initiation and development. Based on the parcel theory of atmospheric convection [27], the buoyancy and vertical motion of air parcels play an essential role in initiating convection. VDRAS outputs, the difference per minute is used in calculating *dR*, *dpt* and *dw*.

As nowcasting is performed on each box, the training data pool is constructed based on the boxes, with the raw 3D data in each box sampled directly as the training dataset. A box is labeled "1" if there is a radar echo $\geqslant$ 35 dBZ in 30 minutes in this box; otherwise this box will be labeled "0". Considering that weather phenomena are continuous in both time and space, we incorporate data from the neighboring eight boxes into the center box in order to account for spatial variability. Each box is 6×6 pixels, so we use an area of 18×18 pixels to allow for spatial variability. There are 20 vertical layers in raw data, so the size of each data sample is $18\times18\times20$. Finally, the total number of data samples is 3,737,332 including both the training and validation datasets.

Four experiments, SBOW, CNN-VR, CNN-V, and CNN-R, were conducted to demonstrate the performance of the CNN-based nowcast method and assess the influence of radar observations and model re-analysis data on the nowcast skill. Here R and V indicate radar and VDRAS, respectively. They are described below:

SBOW: baseline experiment using the machine learning method with the handcraft features described in [12];

CNN-VR: CNN-based nowcast using both 3D radar images and VDRAS fields as input *X*:

$$X = (x_1, x_2, x_3, x_4, x_5, x_6) = (w, dw, pt, dpt, R, dR)$$;

CNN-V: same as CNN-VR but only uses VDRAS fields as input X:

$$X = (x_1, x_2, x_3, x_4) = (w, dw, pt, dpt)$$;and

CNN-R: same as CNN-VR but only uses radar images as input X:

$$X = (x_1, x_2) = (R, dR)$$.

Since the input variables in CNN-V are the same as in SBOW, the CNN-V experiment is used to demonstrate the improvement in skill when using CNN-based deep learning nowcast method over SBOW (which relies on handcraft feature engineering).

C. Cross-Channel 3D Convolution

Each input X contains six coupled physical variables (or channels). These six variables play different roles in convective processes. All variables act together to determine the forecast. Thus, a suitable convolution strategy to convolve different channels is essential. This is fulfilled by cross-channel 3D convolution. The first convolutional layer in our network has 200 kernels. Here, we can establish the following equation:

$$X_k = \mathrm{Re}LU(\sum_j \sum_i W_{ijk} * X_{ij} + b_k), k = 1,\ldots,200$$

where i is the index of channels, j is the index of layers within one channel, and k is the index of feature maps. b_k is the linear bias, X_k is the result feature map, W_{ijk} is the weight matrix, and X_{ij} is the layer j within channel i. An illustration of X_{ij} and W_{ijk} is shown in Fig. 6.

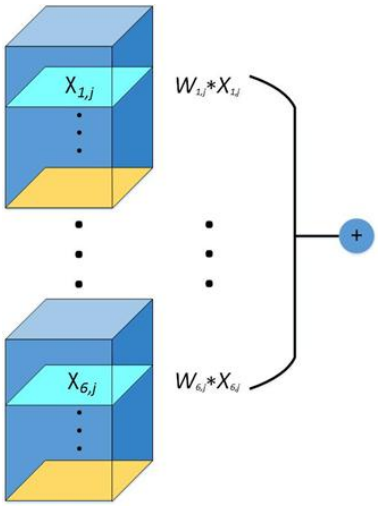

Fig. 6. Illustration of cross-channel 3D convolution.

Because the altitude information of each variable is important, for each fixed altitude or layer, we convolve 2-D layers in different channels to generate a layer-feature map with i. Then, we convolve all 20 layer-feature maps with j to provide an overall feature map. In this way, we accomplish the cross-channel 3D convolution.

IV. Experiments And Analysis

A. Evaluating Metrics

We use the contingency table approach to evaluate the short-term forecasts [28], as is used commonly in weather forecasting community. The probability of detection (POD), false alarm ratio (FAR), and critical success index (CSI) are calculated. POD, FAR, and CSI are similar to precision and recall, which are two skill scores used in the machine-learning field. Schaefer indicates that, for low-frequency events, such as severe weather warnings, CSI is the better choice [29]. POD, FAR, and CSI are defined as:

POD = hits / (hits + misses) = recall

FAR = false alarms / (hits + false alarms) = 1 − precision

CSI = hits / (hits + misses + false alarms)

Here, in each box, a hit occurs when this box is classified as 1 (active) and there is radar echo greater than 35 dBZ in 30 min in the same box (active), a miss occurs when the truth box is active while the forecast box is inactive, and a false alarm occurs when the truth box is inactive while the forecast box is active.

B. Results and Analysis

Table 1 and 2 show the overall POD, FAR, and CSI values for the 30- and 60-minute nowcasts of SBOW, CNN-V, CNN-R and CNN-VR. Note that higher POD, lower FAR, and higher CSI correspond to better skill.

For 30-minute nowcast, CNN-V has a higher CSI value than SBOW (0.41 vs. 0.38), a lower FAR value (0.46 vs. 0.49), and a higher POD value (0.64 vs. 0.62). This indicates that the deep learning method is able to extract more information from the raw VDRAS data compared with SBOW, which results in a superior nowcast. Interestingly, the CNN-R method using only 3D radar reflectivity data alone yields the same CSI value as CNN-V, along with a slightly higher POD value of 0.65. Although VDRAS provides useful atmospheric boundary layer thermal dynamic information, its original resolution is only 3 km compared to the 1 km resolution of radar data. This suggests that the high-resolution raw radar data may have more information than first thought. CNN-R shows an example of exploring such information directly from raw data; notably, this would be difficult for traditional methods.

The best skill (in all three scores) is obtained when both VDRAS re-analysis and radar images are used in CNN-VR. This demonstrates the importance of combining two datasets and shows that our deep learning method can skillfully fuse a multi-source dataset. This result is not surprising, given that the CNN-VR data contain the most recent precipitation and dynamical atmospheric background information (buoyancy and updraft).

Table 1: Skill scores of the four experiments for 30-min forecast

Approach	POD	FAR	CSI
SBOW	0.62	0.49	0.38
CNN-V	0.64	0.46	0.41
CNN-R	0.65	0.47	0.41
CNN-VR	0.69	0.45	0.44

The nowcast skill of the four experiments is better visualized using a performance diagram (as shown in Fig. 7 for 30-minute nowcast case), which combines the three scores and their respective bias scores into a single diagram. Note that the Success Ratio (SR) is equivalent to subtracting FAR from 1, with a perfect nowcast being located at the upper-right corner. Because CNN-VR has a higher CSI, lower FAR (higher SR), and higher POD, it has the best skill (as demonstrated by its close proximity to the upper-right corner). We note that the bias scores of the four experiments are fairly similar, which indicates some over-prediction. All four methods tend to have a slight overforecasting bias, which means they have more false alarms.

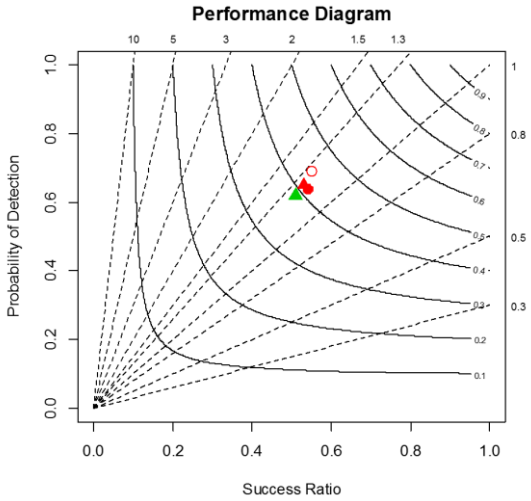

Fig. 7. The performance diagram of SBOW, CNN-VR, CNN-V and CNN-R. Dashed lines represent bias scores with labels on the outward extension of the line, while labeled solid contours are CSI. Four results are shown: SBOW forecasts (bold green triangle), CNN-VR (open red circle), CNN-V forecasts (bold red circle) and CNN-R forecasts (bold red triangle).

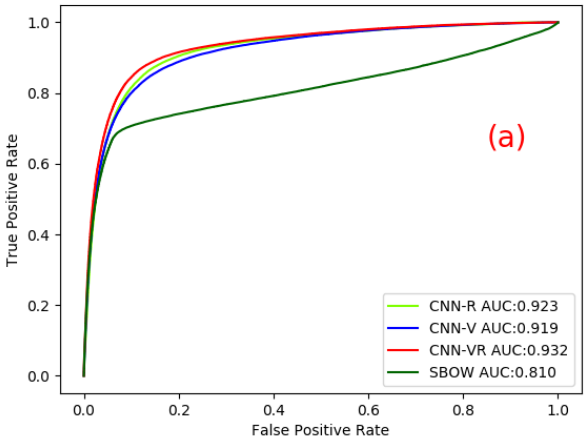

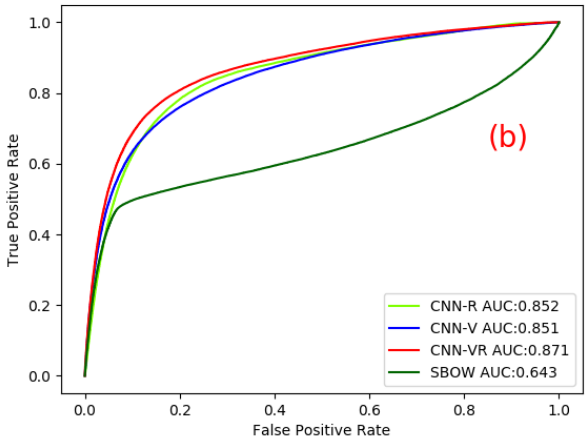

Fig. 8. The ROC curves of four methods. (a). 30-minute nowcast. (b). 60-minute nowcast.

To show how significant the differences were among SBOW, CNN-V, CNN-R, and CNN-VR, we also plotted the receiver operating characteristic (ROC) curves of 30 min and 60 min nowcasts (as shown in Fig. 8). An ROC curve is a graphical plot that illustrates the diagnostic ability of a binary classifier system as its discrimination threshold is varied. The area under the ROC curve (AUC) is one of the most important evaluation metrics for verify-ing the performance of the classification model (i.e., the AUC tells how much a model is capable of distinguishing between classes). The higher the AUC, the better the model is at distinguishing between positive and negative samples. In Figure 8, the AUCs of CNN-VR, CNN-V, and CNN-R were much higher than those of SBOW of both the 30 min and 60 min nowcasts. This showed that the CNN nowcasting methods outperformed SBOW, which is a traditional machine learning method. Among all CNN models, CNN-VR achieved the highest AUC value, which indicated that integrating radar and meteorological re-analysis data was beneficial for nowcasting performance. We further compared the performance of three CNN models on different weather types as follows.

Next, we analyzed the data from convective events in August 2015 that were classified into two categories (Johnson et al. 1998): 1) isolated storm, storm cells are predominantly isolated; and 2) the MCS/Line. Individual storms tend to reside in a large cluster or squall line. Relatively speaking, isolated storms are harder to forecast than MCS/Line storms (Wilson et al. 1998). Tables 2 and 3 show the results for three CNN methods applied to two categories for both 30 min and 60 min forecasts. For every category, CNN-VR had the highest CSI values for 30 min and 60 min forecasts. All skill scores for MCS/Line were better than those for isolated storms.

Figures 9 and 10 show examples of 30 min nowcasts of an isolated storm and a squall line compared with the ground truth (radar reflectivity) at four consecutive times using CNN-VR over the entire study domain. The forecast of CNN-VR was consistent with the real radar echoes.

Table 2. Skill scores of the three experiments for 30-min nowcast.

Approach	POD		FAR		CSI	
	MCS/Line	Isolated	MCS/Line	Isolated	MCS/Line	Isolated
CNN-V	0.70	0.59	0.40	0.57	0.48	0.33
CNN-R	0.74	0.60	0.40	0.59	0.49	0.32
CNN-VR	0.75	0.64	0.39	0.54	0.51	0.36

Table 3. Skill scores of the three experiments for 60-min nowcast.

Approach	POD		FAR		CSI	
	MCS/Line	Isolated	MCS/Line	Isolated	MCS/Line	Isolated
CNN-V	0.62	0.47	0.52	0.74	0.37	0.20
CNN-R	0.58	0.45	0.52	0.75	0.36	0.19
CNN-VR	0.64	0.48	0.48	0.72	0.40	0.22

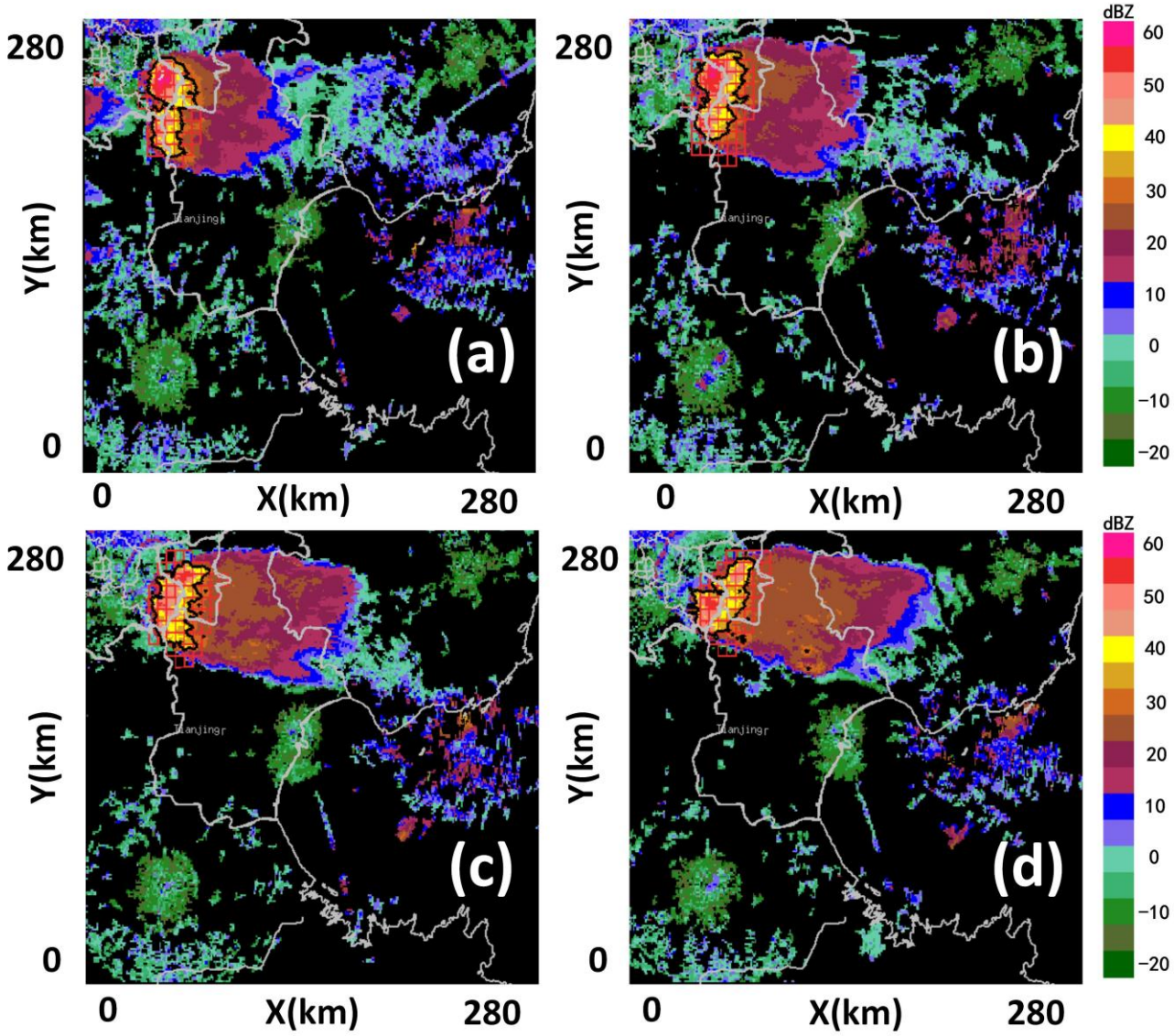

Fig. 9. An example of 30-min nowcasting products of isolated storms compared with the ground truth (radar reflectivity) using CNN-VR at four consecutive times. (a) 09:24 UTC, (b) 09:42 UTC, (c) 10:00 UTC and (d) 10:18 UTC. The red boxes superposed over radar reflectivity represent the 30-min nowcasts, which means there will be a radar echo ≥ 35 dBZ appear in these boxes in 30 minutes. The grey lines indicate province borders. The black curves represent the contours of the 35 dBZ reflectivity level.

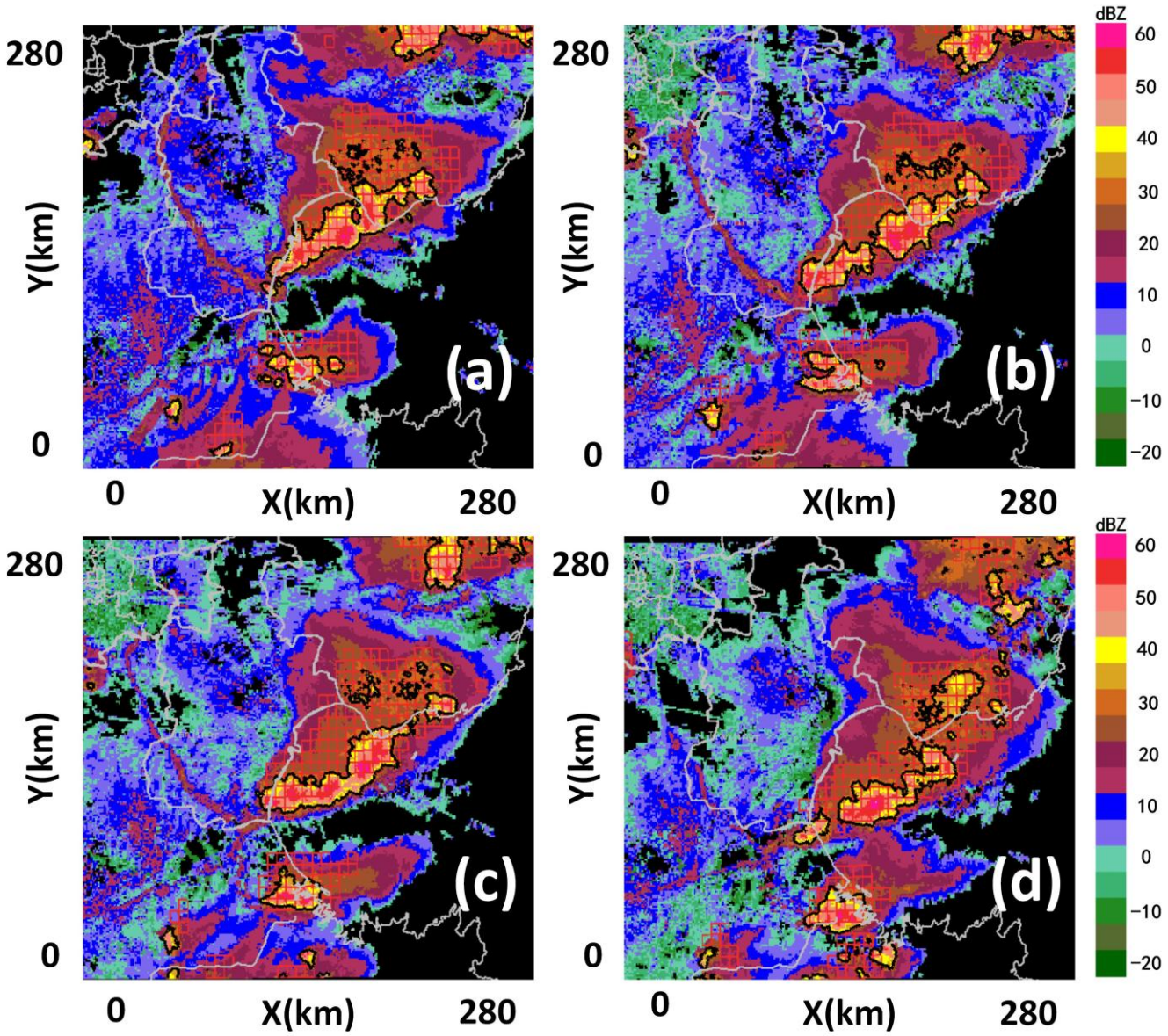

Fig. 10. An example of 30-min nowcasting products of line storms compared with the ground truth (radar reflectivity) using CNN-VR at four consecutive times. (a) 09:03 UTC, (b) 09:20 UTC, (c) 09:38 UTC, (d) 10:08 UTC. The red boxes superposed over radar reflectivity represent the 30-min nowcasts, which means there will be a radar echo ≥ 35 dBZ appear in these boxes in 30 minutes. The grey lines indicate province borders. The black curves represent contours of the 35 dBZ reflectivity level.

V. Discussion And Conclusions

We examined an end-to-end deep learning nowcasting method using 3D radar images and model re-analysis data. The study domain was first divided into position-fixed small boxes and the nowcasting problem was transformed into a single classification problem: will a radar echo ⩾ 35 dBZ appear in a box in 30 or 60 minutes? A deep learning method that uses a convolutional neural network (CNN) was proposed to make predictions. On the first layer of CNN, a cross-channel 3D convolution was constructed to fuse 3D raw data. Unlike traditional machine learning methods, the proposed deep learning nowcasting method eliminates the need for handcraft feature engineering. Next, we evaluated the performance of our deep learning method. In addition, we examined the influence of using radar and re-analysis data on nowcasting skill. Historical data from the Beijing – Tianjin – Hebei region were used to train and test the proposed method. The experimental results demonstrated that deep learning improved the nowcasting skill compared with the traditional method SBOW. While reasonable skill was obtained by using only radar or re-analysis data, the combination of the two datasets resulted in superior performance, which demonstrates the capability of deep learning to fuse multi-source data.

The nowcasting skill may be influenced by the size of the training data, particularly for CI. Due to the short duration and localized CI region (typically only a few grid points), the training data samples for CI constitute only a small proportion of the entire training data pool. Therefore, it is difficult for the deep learning method to retrieve adequate information on CI in order to make accurate predictions. Future work should collect a large number of CI data samples in order to construct a separate CI training data pool. Furthermore, the use of an independently trained classifier may improve the prediction of CI.

ACKNOWLEDGMENT

This work was supported jointly by the National Natural Science Foundation of China (grant numbers 41875049, 41741013), National Key R&D Program of China (grant number 2018YFC1507504-6). We gratefully acknowledge the support of NVIDIA Corporation with the donation of the Tesla GPU used for this research. The data used in this study can be accessed at

http://ihcil.ouc.edu.cn/TGRS2018.html

REFERENCES

[1] Sun J., M.Xue, J. W. Wilson, etc., 2014: Use of NWP for Nowcasting Convective Precipitation: Recent Progress and Challenges. Bull. Amer. Meteor. Soc., 95, 409 – 426.

[2] Joe, P., D. Burgess, R. Potts, T. Keenan, G. Stumpf, and A. Treloar, 2004: The S2K severe weather detection algorithms and their performance. Wea. Forecasting, 19, 43-63.

[3] Wilson, J. W., Y. Feng, and M. Chen, 2010: Nowcasting challenges during the Beijing Olympics: Successes, failures, and implications for future nowcasting systems. Wea. Forecasting, 25, 1691-1714.

[4] Nasrollahi, N., K. L. Hsu, and S. Sorooshian, 2013: An Artificial Neural Network model to reduce false alarms in satellite precipitation products using MODIS and CloudSat observations. J. Hydrometeor., 14, 1872 – 1883.

[5] Sorooshian, S., and Coauthors, 2011: Advanced concepts on remote sensing of precipitation at multiple scales. Bull. Amer. Meteor. Soc., 92, 1353 – 1357.

[6] Tao, Y., X. Gao, K. Hsu, S. Sorooshian, and A. Ihler, 2016: A deep neural network modeling framework to reduce bias in satellite precipitation products. J. Hydrometeor., 17, 931 – 945, doi:10.1175/JHM-D-15-0075.1.

[7] Johnson, J.T., P.L. Mackeen, A. Witt, E.D. Mitchell, G. Stumpf, M.D. Eilts, and K.W. Thomas, 1998: The Storm cell identification and tracking algorithm: an enhanced WSR-88D algorithm. Wea. Forecasting, 13, 263-276.

[8] Dixon, M. and G. Wiener, 1993: TITAN: Thunderstorm identification, tracking, analysis and nowcasting—A radar based methodology. J. Atmos. Oceanic Technol., 10 (6): 785-797.

[9] Tuttle, J.D., and G. B. Foote, 1990: Determination of the boundary layer airflow from a single Doppler radar. J. Atmos. Oceanic Technol., 7, 218-232.

[10] Lai, E.S.T., 1999: TREC application in tropical cyclone observation.Proceedings, ESCAP/WMO Typhoon Committee Annual Review, Seoul, The Typhoon Committee, 135 – 139.

[11] Mueller, C., T. Saxen,R.Roberts, J.Wilson, T. Betancourt, S.Dettling, N. Oien, and J. Yee, 2003: NCAR Auto-Nowcast system. Wea. Forecasting, 18, 545 – 561.

[12] Han L., Sun J., Zhang W., Xiu Y., 2017: A Machine Learning Nowcasting Method based on Real-time Reanalysis Data. J. Journal of Geophysical Research: Atmospheres, 122(7):4038-4051, doi: 10.1002/2016JD025783.

[13] Sun, J. and N. A. Crook, 1997: Dynamical and microphysical retrieval from Doppler radar observations using a cloud model and its adjoint. Part I: Model development and simulated data experiments. J. Atmos. Sci., 54, 1642-1661.

[14] Vincent, P., H. Larochelle, I. Lajoie, Y. Bengio, and P. A. Manzagol, 2010: Stacked denoising autoencoders: Learning useful representations in a deep network with a local denoising criterion. J. Mach. Learn. Res., 11, 3371 – 3408.

[15] Hinton, G. E., Osindero, S. and Teh, Y. W. (2006). A fast learning algorithm for deep belief nets. Neural Computation, 18(7), 1527-1554.

[16] Krizhevsky, A., Sutskever, I., and Hinton, G. E., 2012: Imagenet classification with deep convolutional neural networks. In Advances in neural information processing systems, 1097-1105.

[17] LeCun, Y., Bengio, Y., and Hinton, G., 2015: Deep learning, Nature, 521(1), 436 – 444.

[18] Hinton, G. E. and Salakhutdinov, R. R., 2006: Reducing the dimensionality of data with neural networks. Science, 313(5786), 504-507.

[19] Simonyan, K., and Zisserman., A., 2015: Very deep convolutional networks for large-scale image recognition, International Conference on Learning Representation (ICLR), 1-13.

[20] Sermanet, P., Eigen, D., Zhang, X., Mathieu, M., Fergus, R., & LeCun, Y., 2014: Overfeat: Integrated recognition, localization and detection using convolutional networks, International Conference on Learning Representations (ICLR).

[21] Ren, S., He, K., Girshick, R., & Sun, J., 2015: Faster r-cnn: Towards real-time object detection with region proposal networks. In Advances in neural information processing systems, 91-99.

[22] Tao, Y., X. Gao, K. Hsu, S. Sorooshian, and A. Ihler, 2017:Precipitation Identification with Bispectral Satellite Information Using Deep Learning Approaches. J. Hydrometeor., 18, 1271-1283, doi:10.1175/JHM-D-16-0176.1.

[23] Tao, Y., X. Gao, K. Hsu, S. Sorooshian, and A. Ihler, 2018:A Two-Stage Deep Neural Network Framework for Precipitation Estimation from Bispectral Satellite Information. J. Hydrometeor., 19, 393-408, doi:10.1175/JHM-D-17-0077.1.

[24] Shi, X., Chen, Z., Wang, H., et al., 2015: Convolutional LSTM network: A machine learning approach for precipitation nowcasting. In Advances in neural information processing systems (pp. 802-810).

[25] Chen, M., Y. Wang, F. Gao, and X. Xiao (2012), Diurnal variations in convective storm activity over contiguous North China during the warm season based on radar mosaic climatology, J. Geophys. Res. Atmos., 117, D20115, doi:10.1029/2012JD018158.

[26] Sun, J., M. Chen, and Y. Wang, 2010: A frequent-updating analysis system based on radar, surface, and mesoscale model data for the Beijing 2008 forecast demonstration project. Wea. Forecasting., 25, 1715-1735.

[27] Wallace, J. M. and P. V. Hobbs, 1977: Atmosphere science: an introductory survey, Academic Press, California, USA.

[28] Donaldson, R. J., R. M. Dyer, and M. J. Kraus, 1975: An objective evaluation of techniques for predicting severe weather events. Preprints, Ninth Conf. on Severe Local Storms, Norman, OK, Amer. Meteor. Soc., 321 – 326.

[29] Schaefer, J. T., 1990: The critical success index as an indicator of warning skill, Wea. Forecasting, 5, 570 – 575.